

# Vibrations of a Hollow Nanosphere with a Porous Thin Shell in Liquid

Chengqing Wang<sup>†</sup> and Chi Wu<sup>\*,†,‡</sup>

The Open Laboratory of Bond-Selective Chemistry, Departmental of Chemical Physics, University of Science and Technology of China, Hefei, Anhui, China, 230026, and Department of Chemistry, The Chinese University of Hong Kong, Shatin, N.T., Hong Kong

Received September 3, 2003

Revised Manuscript Received November 2, 2003

Lamb<sup>1</sup> studied the vibrations of an elastic sphere as well as a viscous spheroid more than one century ago. He estimated that for a globe with a size of the earth, the oscillation of longest period was  $1.84 \times 10^{11}$  years and 150 h if the earth was made of water and pitch, respectively. Later, he extended his study to the vibrations of a solid spherical thin shell<sup>2</sup> and found that a thin glass spherical shell (20 cm in diameter) should make  $\sim 5.35 \times 10^3$  vibrations per second in its heaviest mode. At the same time, Rayleigh<sup>3</sup> discussed the flexural vibrations of an open shell or bowl, which is different from a spherical shell because any deformation of a closed convex surface involves extension or contraction in some part of it. Eighty years later, Baker<sup>4</sup> reformulated and extended the ancient studies of Lamb and experimentally confirmed the existence of two different kinds of vibration frequencies (upper and lower branches,  $a_n$  and  $b_n$ ) by studying the vibrations of a large steel shell (30 cm). Both  $a_n$  and  $b_n$  are related to its Poisson ratio ( $\nu \leq 1/2$ ), Young's modulus ( $E$ ), density ( $\rho$ ), and radius ( $R$ ) as

$$a_n = \left[ \frac{E}{2(1-\nu^2)\rho} \right]^{1/2} \frac{f_n^{1/2}}{R} \text{ and } b_n = \left[ \frac{E}{2(1-\nu^2)\rho} \right]^{1/2} \frac{g_n^{1/2}}{R} \quad (1)$$

where  $f_n = [n(n+1) + 1 + 3\nu] + \{[n(n+1) + 1 + 3\nu]^2 - 4(1-\nu^2)[n(n+1) - 2]\}^{1/2}$  and  $g_n = [n(n+1) + 1 + 3\nu] - \{[n(n+1) + 1 + 3\nu]^2 - 4(1-\nu^2)[n(n+1) - 2]\}^{1/2}$ , and  $n$  represents the  $n$ th surface harmonic.

Figure 1 schematically shows different vibration modes on the equator of a hollow sphere, where the wavelength ( $\Lambda$ ) of the  $n$ th surface harmonic is  $2\pi R/n$ . Most of the past studies in this direction were related to macroscopic hollow spheres filled with air, such as music instruments. It has been known that the frequencies increase as  $R$  decreases. There were also studies of the vibration of red blood cells, i.e., the flicker phenomenon.<sup>5–7</sup> For example, Brochard and Lennon<sup>6</sup> studied the frequency spectrum of the flicker phenomenon in erythrocytes by using a phase contrast microscopic method, in which the intensity fluctuations of the light scattered from a single cell were recorded on a magnetic tape and analyzed by the spectrum analyzer. They found that the low frequency of thickness fluctuations is in the range 25–40 Hz. Nowadays, such a measurement can be recorded in time domain in terms of an autocorrelation function, which can measure much higher

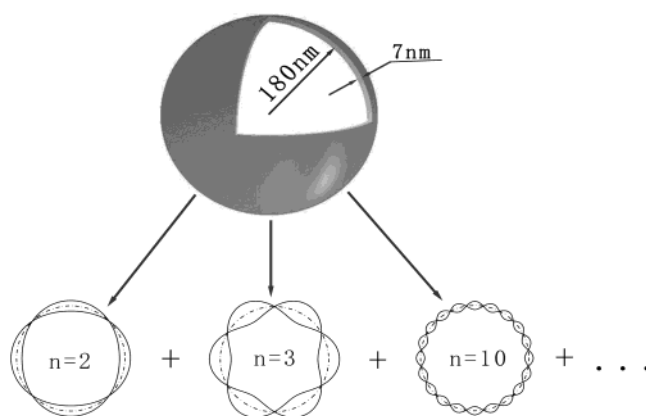


**Figure 1.** Schematic of different vibration (breathing) modes on the equator of an empty hollow sphere with a thin and elastic shell in a vacuum.

frequencies, i.e., smaller hollow spheres. Considering biological cells which have a porous hollow spherical membrane filled with liquid, we decided to prepare narrowly distributed hollow nanospheres ( $\sim 10^2$  nm in size) with a very thin shell made of swollen porous polymer gel and use dynamic laser light scattering (LLS) to study their vibrations in solution. This is because we speculate that such vibrations could affect the transportation of substances in and out of a cell. Here, we would like to report the first observation of vibrations of such hollow nanospheres swollen and suspended in liquid.

To obtain such hollow spheres with a thin wall and a size comparable to the wavelength (532 nm) of the light used in LLS, we first used the seed polymerization to prepare core-shell nanoparticles with the core consisting of un-cross-linked linear poly(methyl methacrylate) (PMMA) and a thin shell made of cross-linked polystyrene (PS). The synthesis detail can be found elsewhere.<sup>8</sup> The outline is as follows. In the preparation of the PMMA seeds (cores), into a 100 mL three-neck flask were added 70 mL of deionized water and 5.0 mL of MMA, and 52 mg KPS as initiator was then added. Nitrogen was bubbled for 30 min to remove the oxygen before the reaction. The reaction lasted 6 h at 70 °C. The shell was prepared by slowly adding a mixture of 1.6 mL of styrene, 1.5 mol % of divinylbenzene as cross-linking agent, and an additional 20 mg of KPS with a syringe pump. After the freeze-drying to remove water, the nanoparticles were placed in toluene, a good common solvent for both PMMA and PS, to form a dilute dispersion ( $1.75 \times 10^{-5}$  g/mL). The swollen porous thin PS shell allowed linear PMMA chains inside to slowly diffuse out after about 1 week time. This was confirmed by a gradual decrease of the scattering intensity when the same hollow spheres were dissolved in THF, another common, but nonisorefractive, solvent, shown in Figure 2. The increase of  $\langle R_g \rangle / \langle R_h \rangle$  from  $\sim 0.8$  to  $\sim 1$  (inset of Figure 2) clearly indicates the change from a uniform solid sphere to a thin hollow shell,<sup>9</sup> where  $\langle R_g \rangle$  and  $\langle R_h \rangle$  are the average radius of gyration and the average hydrodynamic radius, respectively. It is necessary to note that toluene is nearly an isorefractive solvent for PMMA; i.e., individual isorefractive PMMA chains with a relatively low molar mass in solution are invisible in LLS. Such optical invisibility was used before in the

\* The Hong Kong address should be used for correspondence.

<sup>†</sup> University of Science and Technology of China.

<sup>‡</sup> The Chinese University of Hong Kong.

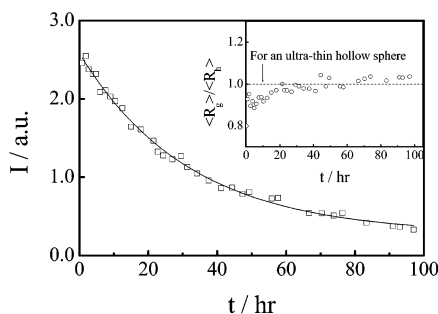


**Figure 2.** Time dependence of scattering intensity ( $I$ ) after the nanoparticles are dispersed and swollen in THF at room temperature, where the inset shows the time dependence of the ratio of average radius of gyration ( $\langle R_g \rangle$ ) to average hydrodynamic radius ( $\langle R_h \rangle$ ) of the nanoparticles. Note that THF is not an isorefractive solvent for the core.

study of ternary polymer solutions.<sup>10–13</sup> Therefore, the most of scattered light come from the thin PS shell, which makes the experiment as well as the data interpretation much easier. This is why we do not have to isolate the hollow spheres from individual chains in dilute dispersion for the present study.

A modified commercial light-scattering spectrometer (ALV/SP-125) equipped with an ALV-5000 multi- $\tau$  digital time correlator was used. In dynamic LLS, the Laplace inversion analysis of the measured intensity–intensity–time correlation function  $G^{(2)}(t)$  led to a line-width distribution ( $G(\Gamma)$ ). For a pure diffusive relaxation,  $\Gamma$  is related to the translational diffusion coefficient ( $D$ ) and the scattering vector ( $q = 4\pi n(\sin \theta)/\lambda_{\text{laser}}$ ) by  $D = (\Gamma/q^2)_{q \rightarrow 0, C \rightarrow 0}$ , where  $n$ ,  $\lambda_{\text{laser}}$ , and  $\theta$  are the refractive index of solvent, laser wavelength, and scattering angle, respectively. It is helpful to note that the reciprocal of  $q$  (i.e.,  $1/q$ ) represents the measurement length in real space. At higher scattering angles, internal motions start to contribute to the spectral distribution ( $S(q, \omega)$ ) of the light scattered from a scattering object. In general,  $S(q, \omega)$  can be written as

$$S(q, \omega) = P_0 \frac{q^2 D}{\pi(\omega^2 + q^2 D)} + \sum_{i=1}^n P_i \frac{q^2 D + \Gamma_i}{\pi(\omega^2 + q^2 D + \Gamma_i)} + \sum_{i=1}^n \sum_{j=1}^n \dots + \sum_{i=1}^n \sum_{j=1}^n \sum_{k=1}^n \dots + \dots \quad (2)$$

where  $\Gamma_i$  represents the line width of the  $\omega$ -normalized Lorentzian distribution related to the  $i$ th normal modes and  $\sum \dots + \sum \sum \dots + \sum \sum \sum \dots + \dots$  represent all the cross terms. The details of the LLS theory and instrumentation can be found elsewhere.<sup>14,15</sup> It is helpful to note that the spectrometer used has a workable low angle range down to  $6^\circ$ , which is vitally important in the measurement of pure translational diffusion of large hollow nanospheres without the interference of internal motions. In a previous parallel experiment, we studied internal motions of long linear PS chains with a size similar to that of the hollow nanospheres used in this study.

Figure 3 shows that when  $x = \langle R_g \rangle q < 1$ ,  $G(\Gamma/q^2)$  has only a single narrowly distributed peak. The  $q$ -independence of the position of this peak indicates that it corresponds to the translational diffusion of hollow nanospheres. As  $q$  increases, the contributions of the second and other high-order terms in eq 2 should broaden this peak when  $(1/q)$  is comparable to  $\langle R_g \rangle$ . Further increase of  $q$  results in a second small peak

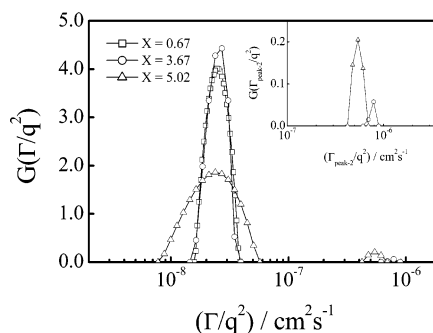


**Figure 3.** Angular dependence of  $q^2$ -normalized line-width distribution ( $G(\Gamma/q^2)$ ) of the thin spherical porous polystyrene shell immersed in toluene, where  $X$  is defined as  $q\langle R_g \rangle$  and the inset shows an enlargement of the second peak related to vibration modes.

which is not related to individual chains because their scattering intensity is more invisible at higher scattering angles. Previous studies of linear chains confirmed that such a second peak is related to internal motions.<sup>16–19</sup> It is helpful to note that in a LLS experiment, we will not be able to resolve each vibration frequency from pure diffusive relaxation ( $(\Gamma)_{\text{peak-1}} = Dq^2$ ) as predicted by eq 2. Instead, we can obtain an average line width ( $(\Gamma)_{\text{peak-2}}$ ) related to internal motions (vibrations or breathing modes). It is also helpful to note that for linear chains internal motions start to appear in  $G(\Gamma)$  when  $q\langle R_g \rangle \sim 1$ . While for hollow nanospheres, the second peak appears only when  $\langle R_g \rangle q \sim 3.7$ , i.e.,  $1/q = \langle R_g \rangle / 3.7 \approx 47$  nm. This reveals that the slowest “breathing” mode of a linear chain is related to the motion of involve the entire chain, but the slowest observable vibration of a porous spherical shell immersed in liquid involves only a portion of the shell. In other words, the vibrations with a wavelength longer than  $\sim 47$  nm cannot be detected in LLS. It seems that the hollow nanosphere is not able to deform into an ellipse or “breathing”, as shown in Figure 1, when  $n (= 2\pi R/\lambda)$  is less than 24. This could be understood when we consider the surface movements of a small pond. Normally, we do not see the up and down of the entire surface of the pond, but only small surface waves. Of course, a small pond is very different from the hollow nanospheres studied here. Theoretically, it has been shown that the lowest relaxation mode of vesicles vanishes when the shell is not sufficiently soft.<sup>20</sup>

Note that in eq 1, the Young’s modulus ( $E$ ) of a swollen polymer gel can be related to its dried density ( $\rho_{\text{dry}}$ ), the average molar mass ( $M_c$ ) of the chain segments between two neighboring cross-linking points, and the volume ratio ( $V_{\text{dry}}/V_{\text{swollen}}$ ) of the gel before and after the swelling as  $E = (3k_B T \rho_{\text{dry}}/M_c)(V_{\text{dry}}/V_{\text{swollen}})$ .<sup>21</sup> Since  $\rho_{\text{dry}} V_{\text{dry}} = \rho_{\text{swollen}} V_{\text{swollen}} = W_{\text{gel}}$  (the weight of the polymer gel network), eq 1 can be rewritten as

$$a_n = \left[ \frac{3k_B T}{2(1 - \nu^2)M_c} \right]^{1/2} \frac{f_n^{1/2}}{R} \quad \text{and} \quad b_n = \left[ \frac{3k_B T}{2(1 - \nu^2)M_c} \right]^{1/2} \frac{g_n^{1/2}}{R} \quad (3)$$

For a given hollow sphere with a shell made of a swollen gel, both  $R$  and  $M_c$  are constants. When  $n$  is sufficiently larger,  $f_n$  becomes proportional to  $n$  and  $g_n$  approaches a constant. Therefore, the vibration frequency (here is

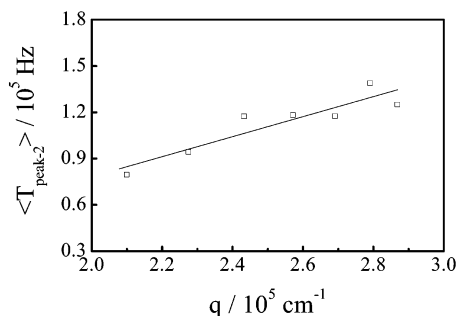


**Figure 4.** Scattering vector dependence of average line-width ( $\langle \Gamma_{\text{peak-2}} \rangle$ ) of the second peak (in Figure 3) of the thin spherical porous polystyrene shell immersed in toluene. The line is just to guide the eye.

related to  $\Gamma$ ) is proportional to  $n$  when  $n \gg 1$ . Since the reciprocal of  $q$  is related to the wavelength of surface wave ( $\Lambda$ ), i.e.,  $1/q \sim \Lambda = 2\pi R/n$ . Therefore,  $\Gamma \propto n \sim q$ , which is what we have observed in Figure 4. However, it should be noted that  $\langle \Gamma_{\text{peak-2}} \rangle$  is in the range of  $8 \times 10^4$ – $1.4 \times 10^5$  Hz, several orders of lower than  $a_n$  and  $b_n$  predicted by eq 3 if we put in  $T = 298$  K,  $0 < \nu < 1/2$ ,  $M_c \sim 1500$  g/mol, and  $R \sim 180$  nm. It is not so surprising to see such a difference because eq 3 was derived for a solid and elastic spherical shell in a vacuum. In the present case, the hollow nanosphere was filled and immersed in viscous liquid and the shell is porous so that solvent can go in and out when it vibrates. It is expected that viscous liquid will damp the vibration. At this moment, the exact formulation of vibrations of such a hollow sphere immersed in liquid is still missing.

**Acknowledgment.** The financial support of the Hong Kong Special Administration Region Earmarked Grants (CUHK4025/02P, 2160181), the NNSF project

(29974027), and the Special Funds for Major State Basic Research Projects (G1999064800) is gratefully acknowledged.

**Supporting Information Available:** Figure showing fittings of two  $(qR)^2$  scaled structural factors of thin-shell hollow spheres with different radii. This material is available free of charge via the Internet at <http://pubs.acs.org>.

## References and Notes

- (1) Lamb, H. *Proc. London Math. Soc.* **1881**, *13*, 51 and 189.
- (2) Lamb, H. *Proc. London Math. Soc.* **1882**, *14*, 50.
- (3) Rayleigh, L. *Proc. London Math. Soc.* **1881**, *13*, 4.
- (4) Baker, W. E. *J. Acous. Soc. Am.* **1961**, *33*, 1749.
- (5) Blowers, R.; Clarkson, E. M.; Maizals, M. *J. Physiol.* **1950**, *113*, 228.
- (6) Brochard, F.; Lennon, J. F. *J. Phys. (Paris)* **1975**, *36*, 1035.
- (7) Tishler, R. B.; Calson, F. D. *Biophys. J.* **1993**, *65*, 2586.
- (8) Jönsson, J. E.; Hassander, H.; Toernell, B. *Macromolecules* **1994**, *27*, 1932; Jönsson, J. E.; Karlsson, O. J.; Hassander, H.; Törnell, B. *Macromolecules* **2001**, *34*, 1512.
- (9) Burchard, W. *Light Scattering Principles and Development*; Clarendon Press: Oxford, England, 1996.
- (10) Wheeler, L. M.; Lodge, T. P. *Macromolecules* **1989**, *22*, 3399.
- (11) Sun, Z.; Wang, C. H. *Macromolecules* **1996**, *29*, 2011.
- (12) Pinder, D. N. *Macromolecules* **1997**, *30*, 226.
- (13) Ohshima, A.; Sato, T.; Teramoto, A. *Macromolecules* **2000**, *33*, 9769.
- (14) Chu, B. *Laser Light Scattering*, 2nd ed.; Academic Press: New York, 1991.
- (15) Berne, B.; Pecora, R. *Dynamic Light Scattering*; Plenum Press: New York, 1976.
- (16) Han, C. C.; Akcasu, A. Z. *Macromolecules* **1981**, *14*, 1080.
- (17) Nemoto, N.; Makita, Y.; Tsunashima, Y.; Kurata, M. *Macromolecules* **1984**, *17*, 425.
- (18) Chu, B.; Wang, Z.; Xu, J. *Macromolecules* **1991**, *24*, 6832.
- (19) Wu, C.; Chan, K. K.; Xia, K. Q. *Macromolecules* **1995**, *28*, 1032.
- (20) Milner, S. T.; Safran, S. A. *Phys. Rev. A* **1987**, *36*, 4371.
- (21) Munk, P. *Introduction to Macromolecular Science*; John Wiley & Sons, Inc.: 1989.

MA035301I